Environmental Earth Sciences (2026) 85:358
https://doi.org/10.1007/s12665-026-13103-z

ORIGINAL ARTICLE

The impact of climate change on the river basins of Parma (Italy) and Kamianka (Ukraine): a comparative analysis

Hanna Kireitseva[1] · Olha Shomko[2] · Iryna Davydova[1] · Elena Maestri[2]

Received: 21 January 2026 / Accepted: 3 August 2026
© The Author(s) 2026

Abstract
This study compares climate change impacts on two contrasting European river basins: the Parma River (Italy) and the Kamianka River (Ukraine) representing different ecoregions and climatic zones. The research used QGIS tools and satellite data from Landsat Collection 2 Level 2 from 1990, 2000, 2010, 2020 and 2023 years to analyze temporal vegetation and water index changes. The methodology incorporated normalized difference vegetation index (NDVI) and normalized difference water index (NDWI) calculations, along with an analysis of temperature trends and standardized precipitation index (SPI-6) data. Results revealed distinct patterns of climate change impacts: the Parma River basin experienced a temperature increase of 1.03°C during 1990–2020 with dominant NDVI class intervals in the 0.3 to 0.6 range in 2010–2020, while dominant NDWI class intervals remained negative (-0.3 to -0.2) with the driest conditions around 2000. The Kamianka River basin showed a more pronounced temperature rise of 1.4°C with dominant NDVI class intervals increasing after 2000 up to range 0.4 to 0.6 and dominant NDWI class intervals shifting toward more negative values (-0.3 to -0.2), suggesting increased water stress. Both basins exhibited different vulnerability patterns: the Parma River system faces increased flood risks and potential agricultural productivity gains. In contrast, the Kamianka River system shows heightened drought susceptibility and potential agrarian productivity losses. These findings suggest the need for tailored adaptation strategies for river basin management under different climatic conditions.

Keywords Climate change · River ecosystems · Environmental monitoring · Water resources · Ecological safety · Remote sensing

Introduction

Climate change poses a growing global threat to ecological systems, with river basins particularly vulnerable due to their sensitivity to both climatic and anthropogenic pressures (Arnell and Gosling 2016; Wang et al. 2024). These impacts span ecological, hydrological, and socio-economic dimensions, necessitating sustainable management strategies adapted to local contexts.

Understanding these complex interactions requires systematic research across different geographical and climatic contexts. Over the past decade, scientists have employed various methodologies and tools to analyze how river systems respond to climate change, leading to significant advances in our knowledge of these dynamics. These studies have not only improved our understanding of river system vulnerabilities but have also highlighted the importance of regional specificity in climate change impacts.

✉ Elena Maestri
elena.maestri@unipr.it

Hanna Kireitseva
gef_kgv@ztu.edu.ua

Olha Shomko
olha.shomko@unipr.it; olya.shomko@gmail.com

Iryna Davydova
div@ztu.edu.ua

[1] Department of Ecology and Environmental Technologies, Zhytomyr Polytechnic State University, 103 Chudnivska St, Zhytomyr 10009, Ukraine

[2] Department of Chemistry, Life Sciences and Environmental Sustainability, University of Parma, Podere Ambolana Moroni, Parco Area delle Scienze, 33/A, Parma 43124, Italy

Published online: 07 August 2026

Recent research demonstrates the complex nature of climate change impacts on river systems across different ecoregions and climatic zones. Studies emphasize regional variability in climate impacts. Parajka et al. (2013) found that hydrological models perform better in humid areas, while Ranjbar et al. (2018) noted greater heterogeneity in dry basins.

The advancement of Geographic Information Systems (GIS) and satellite technology has revolutionized river monitoring capabilities. Nones (2021) and Langat et al. (2019) demonstrated the effectiveness of these technologies in evaluating river channel evolution through morphological monitoring, particularly in studies of the Vistula River in Poland and the Tana River in Kenya. The development of specialized tools like River Metrics has enhanced our ability to analyze river changes through indices such as sinuosity and braiding (De Rosa et al. 2024).

Comparative research by Wang et al. (2017) and Hattermann et al. (2017) showed that regional models better capture local responses to climate stress, reinforcing the importance of ecoregion-specific analysis. The application of the NDVI, which reflects the density and condition of the vegetation cover, and of the NDWI, which indicates the presence of moisture or water in vegetation and on the land surface, has become crucial in monitoring river ecosystem changes. Gogoi and Rawat (2024) used these indices in the Gai River basin (India) to track changes in vegetation and water resources over time. Similarly, Lu et al. (2021) employed NDVI to analyze the relationship between vegetation changes and climate factors in the Yellow River Basin (China), revealing positive correlations over 30 years.

Satellite altimetry has emerged as a valuable tool for monitoring water levels, particularly in remote areas. Jarihani et al. (2013) and Sulistioadi et al. (2015) demonstrated their effectiveness in monitoring hydrodynamic behavior and simulating flood events, though challenges remain in accurately measuring smaller water bodies due to resolution limitations. The integration of citizen science through platforms like Google Earth Engine (Abdelkader et al. 2024) has helped enhance data accuracy and fill observational gaps.

Climate change impacts are particularly pronounced in certain regions. Pechlivanidis et al. (2017) found that impacts are more severe in dry regions, especially toward the end of the century. This finding aligns with Chen et al. (2019) global analysis of river topography, which showed that aridity significantly influences river profiles, with increased straightness in more arid conditions.

Despite these advances, there remains a clear gap in comparative studies across European ecoregions especially between Mediterranean and Eastern European River basins, where contrasting climate regimes and environmental stressors may lead to distinct ecosystem responses. However, as Heidari et al. (2020) emphasize, even basins with similar landforms may respond differently due to climatic variability, underlining the importance of geographically specific research. Additionally, while GIS and satellite data analysis have proven effective in river monitoring, their application in cross-regional comparative studies has been limited.

This comparative study aims to highlight how different climatic conditions affect river ecosystems over time. By focusing on two representative basins from contrasting European ecoregions – the Italian-Corsican and the Eastern European Plains – this research addresses the need for region-specific insights into climate change impacts.

Although remote sensing provides an effective tool for long-term environmental monitoring, interpretation of vegetation and moisture indices should consider possible influences of land-use changes, vegetation dynamics, and methodological uncertainties. Therefore, the present study focuses on identifying climatic relationships while acknowledging this potential limitation.

Methods

A comprehensive methodological framework was developed for the comparative analysis using QGIS tools and satellite data from several sources (Fig. 1). The study was based on satellite imagery data from the USGS Landsat Collection 2 Level 2 (USGS, 2024) for five time periods: 1990, 2000, 2010, 2020 and 2023. For each of the selected years, three cloud-free images were selected, one for each season: spring, summer, autumn. The seasons were defined as spring (March–May), summer (June–August), and autumn (September–November). This resulted in a total of 30 images, 15 for the Parma and 15 for the Kamianka River basins.

The satellite images were obtained from various Landsat missions: Landsat 4–5 TM for 1990 and 2010, Landsat 7 ETM+for 2000, and Landsat 8–9 OLI/TIRS for 2020 and 2023. The analysis used the main spectral channels: green (0.52–0.60 µm), red (0.63–0.69 µm) and near-infrared (NIR, 0.76–0.90 µm) with a spatial resolution of 30 m. NDVI was calculated based on the red and NIR channels (Bands 4 and 5 for Landsat 8–9; Bands 3 and 4 for previous missions). NDWI was calculated using the green and NIR channels (Bands 3 and 5 for Landsat 8–9; Bands 2 and 4 for previous missions). These spectral ranges were chosen because of their high sensitivity for detecting vegetation cover and water bodies.

The key stages of the study are band selection, raster calculation (NDVI/NDWI), vector layer creation, clipping and styling of raster layers, DEM visualization, and

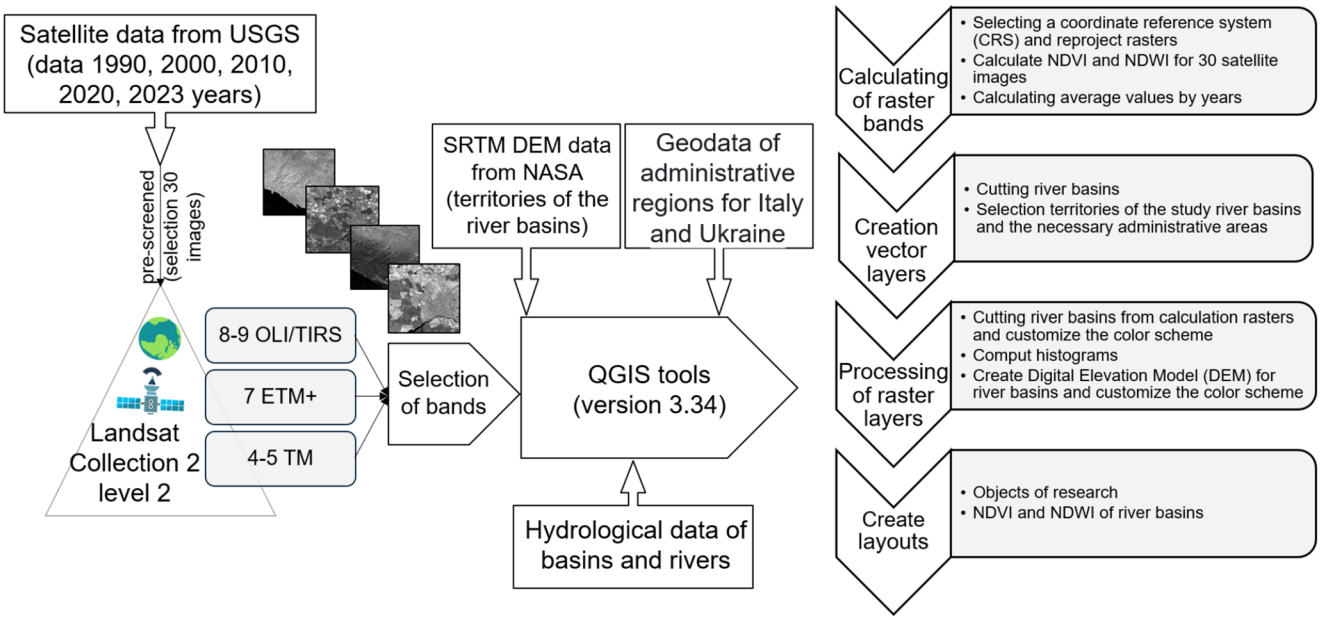

Fig. 1 Methodological framework for processing satellite data and spatial analysis. The diagram outlines the workflow used for analyzing NDVI and NDWI based on Landsat Collection 2 Level 2 satellite imagery. A total of 30 cloud-free images were pre-selected from Landsat sensors. Additional input data included SRTM digital elevation models (DEM), administrative boundaries for Italy and Ukraine, and hydrological vector data

layout generation. Data processing was performed in QGIS (version 3.34). For each year, NDVI and NDWI indices were calculated separately for each seasonal image using the Raster Calculator. The NDVI is calculated using formula 1 (EOS 2024):

$$\mathrm{NDVI} = \frac{(\mathrm{NIR\text{-}RED})}{(\mathrm{NIR} + \mathrm{RED})} \tag{1}$$

where: NIR – reflectance in the near-infrared range, RED – reflectance in the red range.

The NDVI values range from −1 to +1, with higher values indicating denser and healthier vegetation. Similarly, the NDWI is calculated as formula 2 (EOS 2024):

$$\mathrm{NDWI} = \frac{(\mathrm{Green\text{-}NIR})}{(\mathrm{Green}+\mathrm{NIR})} \tag{2}$$

where: Green – reflectance in the green range, NIR – reflectance in the near-infrared range.

The NDWI values also range from −1 to +1, with higher values indicating greater water presence. The annual seasonal-mean index value was calculated using the formula 3:

$$\mathrm{I_{year}} = \frac{(\mathrm{I_{spring}}+\mathrm{I_{summer}}+\mathrm{I_{autumn}})}{3} \tag{3}$$

where: $\mathrm{I_{year}}$ – annual seasonal-mean index value for the corresponding year, $\mathrm{I_{spring}}$ – index value (NDVI or NDWI) for the spring image, $\mathrm{I_{summer}}$ – index value for the summer image, $\mathrm{I_{autumn}}$ – index value for the autumn image.

Annual seasonal-mean NDVI and NDWI rasters were produced for each year as the mean of the three seasonal index maps (spring, summer and autumn). For basin-level reporting, raster histograms were generated in QGIS, and the dominant class interval was identified as the interval corresponding to the highest-frequency peak of the pixel-value distribution within each basin.

The dominant class interval was chosen as a descriptive indicator because it reflects the range of pixel values that occurs most frequently within each river basin and is less sensitive to local outliers than minimum or maximum values. This approach allows for a consistent comparison of prevailing vegetation and moisture conditions across different years, while avoiding overinterpretation of isolated extreme values. Hydrological data for basins and river contours, as well as their shapefiles, were obtained from BasinATLAS and RiverATLAS datasets provided by HydroSHEDS (HydroSHEDS 2024). The resulting raster images were clipped to the boundaries of the respective river basins in QGIS using the “Clip Raster by Mask Layer” tool with vector polygons of the basin contours. At the final stage, each index layer was visualized using the Singleband pseudocolor symbology. Fixed classification intervals and a unified color scale were

applied to ensure the comparability of results in space and time. This approach enabled clear identification of spatial changes in vegetation cover and water balance within the selected basins. Additionally, we used SRTM DEM data from NASA 2024 for terrain visualization, geodata of administrative regions for Italy and Ukraine (FAO 2024; Geoportal 2024).

Methodological limitations

The study includes several methodological limitations. First, the temporal comparison was based on five representative years of observations rather than continuous annual monitoring, which limits the statistical reliability of the analysis of long-term trends. Second, the NDVI and NDWI indices are indirect indicators of vegetation cover and surface moisture and may also be influenced by changes in land use, agricultural practices, vegetation structure, and seasonal variability. Third, the ERA5 reanalysis data provide spatially interpolated climate estimates and may differ from local ground-based observations. Finally, the correlation analysis is exploratory in nature due to the limited number of observations and should therefore be interpreted with appropriate caution.

Results

Geospatial characteristics and Digital Elevation Models (DEM)

For comparative analysis, two river basins from different ecoregions were selected. Both river basins have unique relief characteristics and elevation distribution, as shown in their DEMs. The first study area is the Parma River basin, located in the Emilia-Romagna region, Italy (Fig. 2).

In additional to the Parma River basin, the second study area is the Kamianka River basin, located in the Zhytomyr region, Ukraine (Fig. 3).

The Parma River basin (Fig. 2) is characterized by significant elevation changes ranging from 0 to 1,755 m above sea level, which is typical for the Apennine foothills. In contrast, the Kamianka River basin (Fig. 3) is located within the East European Plain with less pronounced relief and elevations ranging from 179 to 256 m above sea level. The DEM demonstrates how these contrasting topographical settings influence their hydrological responses to climate change, with the steeper gradients of the Parma River basin suggesting different runoff patterns and erosion processes compared to the more gradual slopes of the Kamianka River basin.

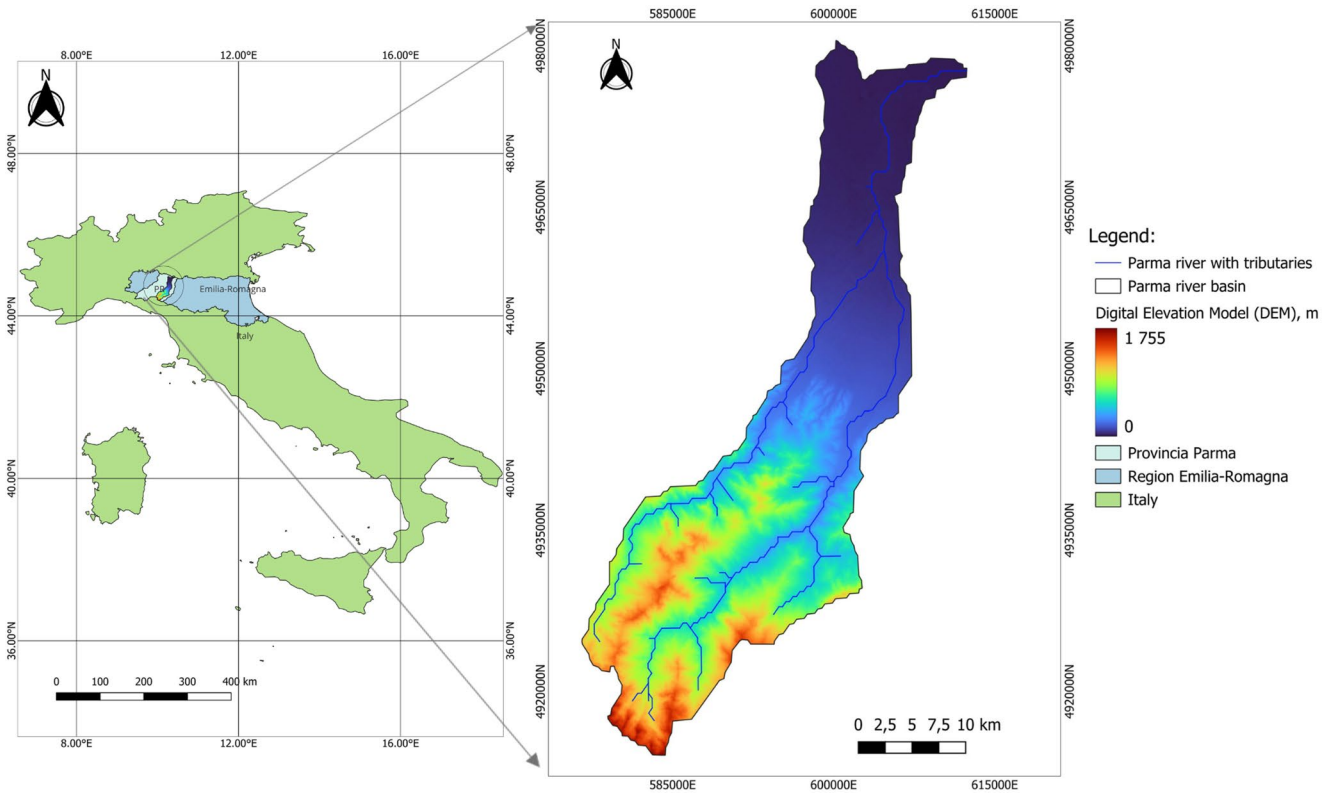

Fig. 2 Geographic location and digital elevation model (DEM) of the Parma River basin: the left panel shows the location of the basin within Italy and the Emilia-Romagna region, highlighting administrative boundaries; the right panel presents the DEM of the basin, with elevation ranging from 0 to 1755 m, derived from (NASA 2024)

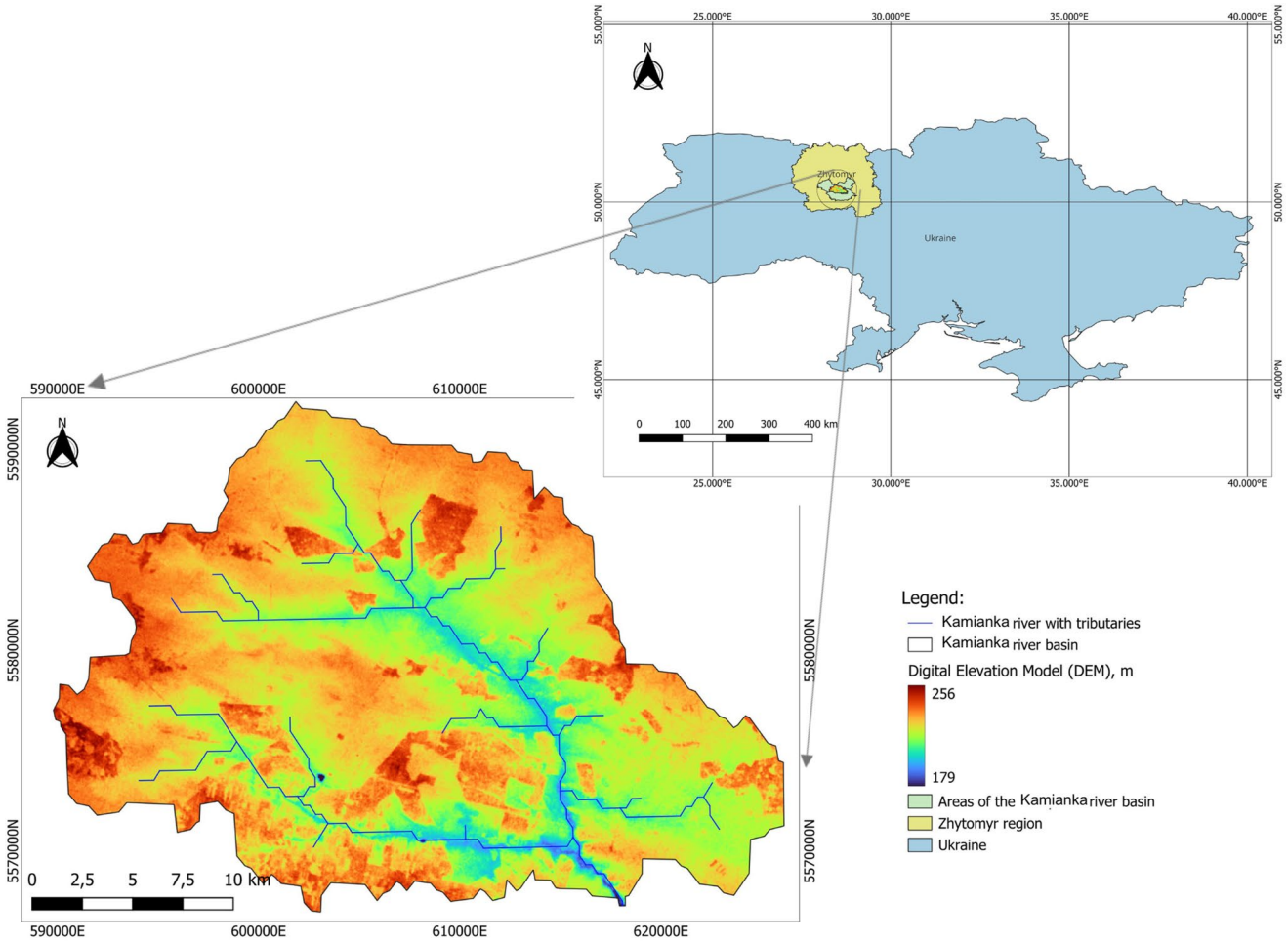

Fig. 3 Geographic location and digital elevation model (DEM) of the Kamianka River basin (Zhytomyr region, Ukraine). The upper right corner shows the location of the basin within Ukraine and the Zhytomyr administrative region. The main panel presents the DEM of the basin, with elevation ranging from 179 to 256 m derived from (NASA 2024). The map shows the river network and tributaries of the Kamianka River, as well as the boundaries of the basin.

Table 1 Comparative analysis of parameters and characteristics of the Parma and Kamianka rivers

Parameter/Characteristic	Parma river (Italy)	Kamianka river (Ukraine)
Length	92 km	32 km
Basin area	796 km²	602 km²
Ecoregion (according to WFD)	Italian-Corsican (9)	Eastern Plains (16)
Water body type	River	River
Altitude typology	Mid-altitude (200–800 m)	Lowland (<200 m)
Basin size (according to WFD)	Medium (>100–1000 km²)	Medium (>100–1000 km²)
Feeding regime	Mixed	Mixed
Use for drinking water supply	No	No
Anthropogenic load	Moderate	Moderate

WFD stands for Water Framework Directive (WFD 2024)

A detailed comparison of these rivers reveals both similarities and distinct characteristics that make them particularly suitable for comparative climate change impact analysis (Table 1).

While the Parma River is significantly longer, with a length of 92 km, compared to the Kamianka River, which stretches 32 km, both basins fall within the medium size category between 100 and 1000 km², in accordance with the Water Framework Directive (WFD) classification, with areas of 796 km² and 602 km² respectively.

The rivers belong to different ecoregions – Italian-Corsican for Parma River and Eastern Plains for Kamianka River

– and altitude typologies, with Parma River characterized as mid-altitude and Kamianka River as lowland. Despite these geographical differences, both rivers share similar characteristics in terms of their feeding regime, and anthropogenic load, and neither is used for drinking water supply. This combination of shared characteristics and distinct geographical features makes these river basins valuable for studying how similar anthropogenic pressures and climate change impacts manifest differently across varied European ecoregions.

Comparative analysis of NDVI and NDWI seasonal dynamics

The NDVI values range from −1 to +1, with higher values indicating a greater presence of vegetation. For the classification of the study area, NDVI values were divided into six classes: values≤0 indicate water bodies, snow, ice, or clouds; 0 to 0.1 correspond to bare rocks, sand, or urban areas; 0.1 to 0.2 reflect sparse vegetation or agricultural land with low vegetation; 0.2 to 0.3 represent shrubs and grasslands; 0.3 to 0.6 indicate dense herbaceous vegetation or forests; and values>0.6 denote dense, healthy vegetation such as crops at their peak growth.

The NDWI values were similarly categorized: values ≤ −0.5 represent non-aqueous surfaces under drought conditions; −0.5 to −0.3 correspond to drought-affected non-aqueous areas; −0.3 to 0 indicate moderate drought; 0 to 0.2 reflect built-up features, flooding, or humidity; 0.2 to 0.5 represent typical water surfaces; and values>0.5 are associated with open water bodies.

Based on these defined thresholds, the analysis of seasonal dynamics during the 2023 growing season revealed distinct patterns in vegetation coverage and water content for both river basins. Figure 4 presents the comparative analysis of seasonal dynamics during the growing season in 2023, which revealed distinct patterns in vegetation coverage and water content for both river basins. In the Parma River basin (Fig. 4, a), NDVI values demonstrated consistent moderate to high vegetation density, with values ranging from 0.2 to 0.5 and peak frequencies around 0.4. This distribution suggests healthy vegetation conditions throughout the growing season. The NDWI analysis revealed dry conditions, with values primarily falling between −0.4 and −0.2, indicating limited surface water presence outside the main river channel.

The Kamianka River basin (Fig. 4, b) exhibited similar vegetation patterns but with slightly distinct characteristics. The NDVI values peaked at around 0.3, with most readings falling between 0.2 and 0.4, indicating good vegetation conditions and moderate photosynthetic activity across all seasons. The NDWI values for the Kamianka River basin showed comparable dry conditions to the Parma River basin, with predominant values ranging from −0.4 to −0.2, suggesting low water content in vegetation and soil despite different geographical and climatic contexts.

These seasonal dynamics, visualized through both distribution maps and corresponding histograms, demonstrate that despite their different ecoregional settings, both river basins maintained stable vegetation conditions throughout the 2023 growing season while experiencing similarly dry conditions in terms of water content.

To capture longer-term changes, we compared basin conditions across five representative time points (1990, 2000, 2010, 2020 and 2023). The year 1990 was used as the baseline for assessing decadal-scale changes in vegetation and surface water conditions.

As shown in Fig. 5, a long-term analysis of the Parma River basin, based on annual seasonal-mean NDVI and NDWI rasters derived from three cloud-free Landsat images for each year (spring, summer, autumn; see Methods), reveals marked variability across the selected observation years (1990, 2000, 2010 and 2020), reflecting decadal-scale changes in vegetation cover and surface water conditions. Variations in NDVI values show notable fluctuations, with the most robust vegetation conditions observed in 1990 (predominantly values between 0.3 and 0.6, indicating dense vegetation and healthy forests). A noticeable decrease in vegetation density was recorded in 2000, as evidenced by lighter green tones in the NDVI map and a shift in histogram peaks toward lower values. The basin showed signs of recovery in 2010 and 2020, though not reaching the 1990 levels of vegetation density.

The NDWI patterns for the Parma River basin demonstrate a consistent trend toward drier conditions. The 1990 data show more varied water content distribution, with some areas displaying values between −0.3 and 0, indicating moderate moisture levels. However, subsequent decades show a progressive shift toward drier conditions, particularly evident in the 2020 data where larger areas exhibit NDWI values below −0.3, suggesting increased water stress in the basin.

The analysis of the Kamianka River basin (Fig. 6) show different patterns of change across the selected observations, years. The NDVI analysis reveals more stable vegetation conditions with values consistently ranging between 0.2 and 0.4, indicating moderate vegetation health. The histograms show a consistent pattern across all four time periods, though with subtle shifts in peak values. Data for 2010 and 2020 suggest a slight decline in vegetation density compared to 1990 levels, but the changes are less pronounced than those observed in the Parma River basin.

The NDWI dynamics in the Kamianka River basin show a gradual trend toward drier conditions, particularly evident

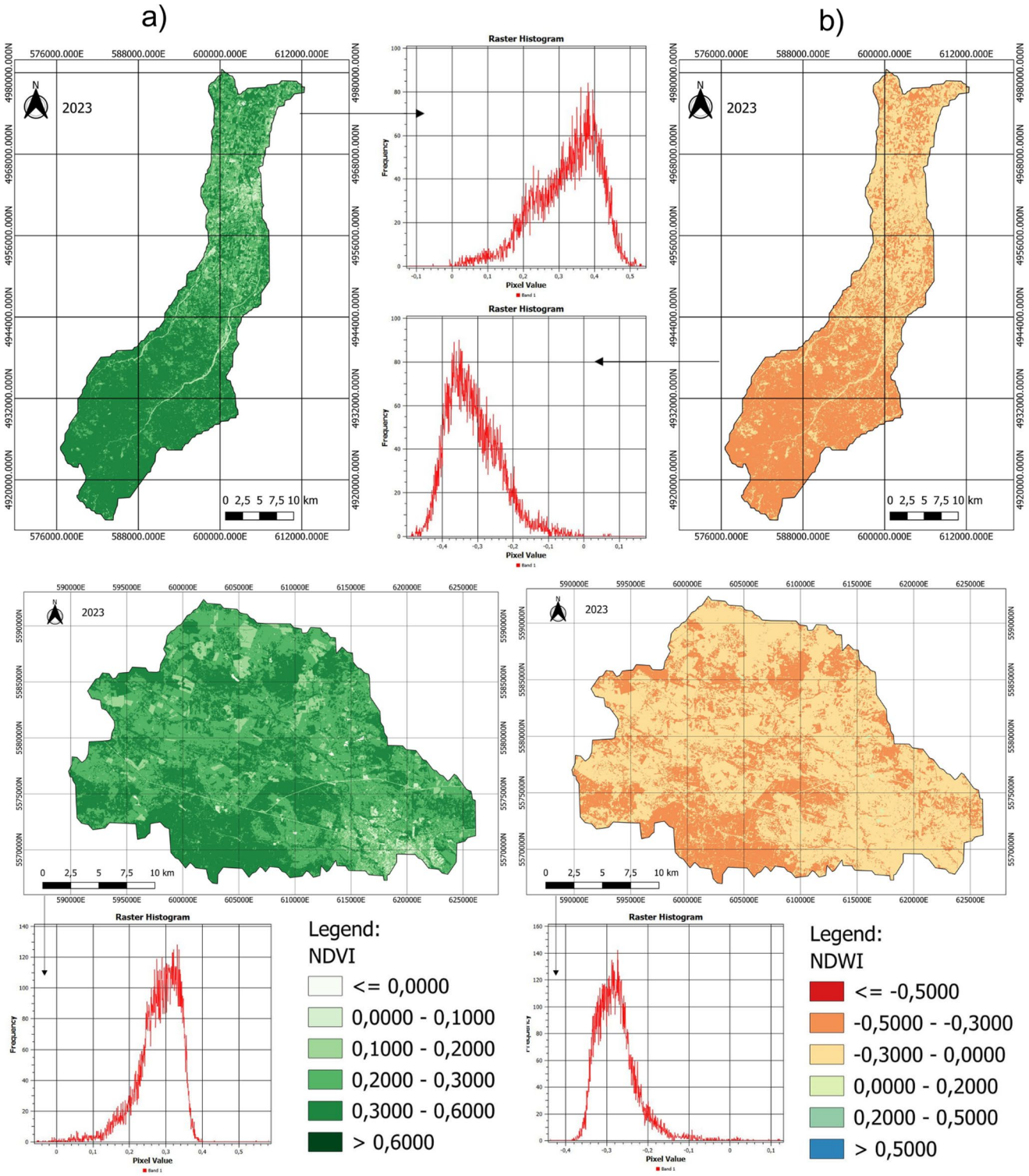

Fig. 4 Comparative analysis of NDVI and NDWI seasonal dynamics in the Parma and Kamianka River basins for the year 2023: a – shows the spatial distribution of the NDVI for the Parma (top) and Kamianka (bottom) River basins, highlighting vegetation density and heterogeneity; b – presents the corresponding distribution of the NDWI, reflecting surface water content. Raster histograms illustrate the frequency distribution of pixel values across each basin

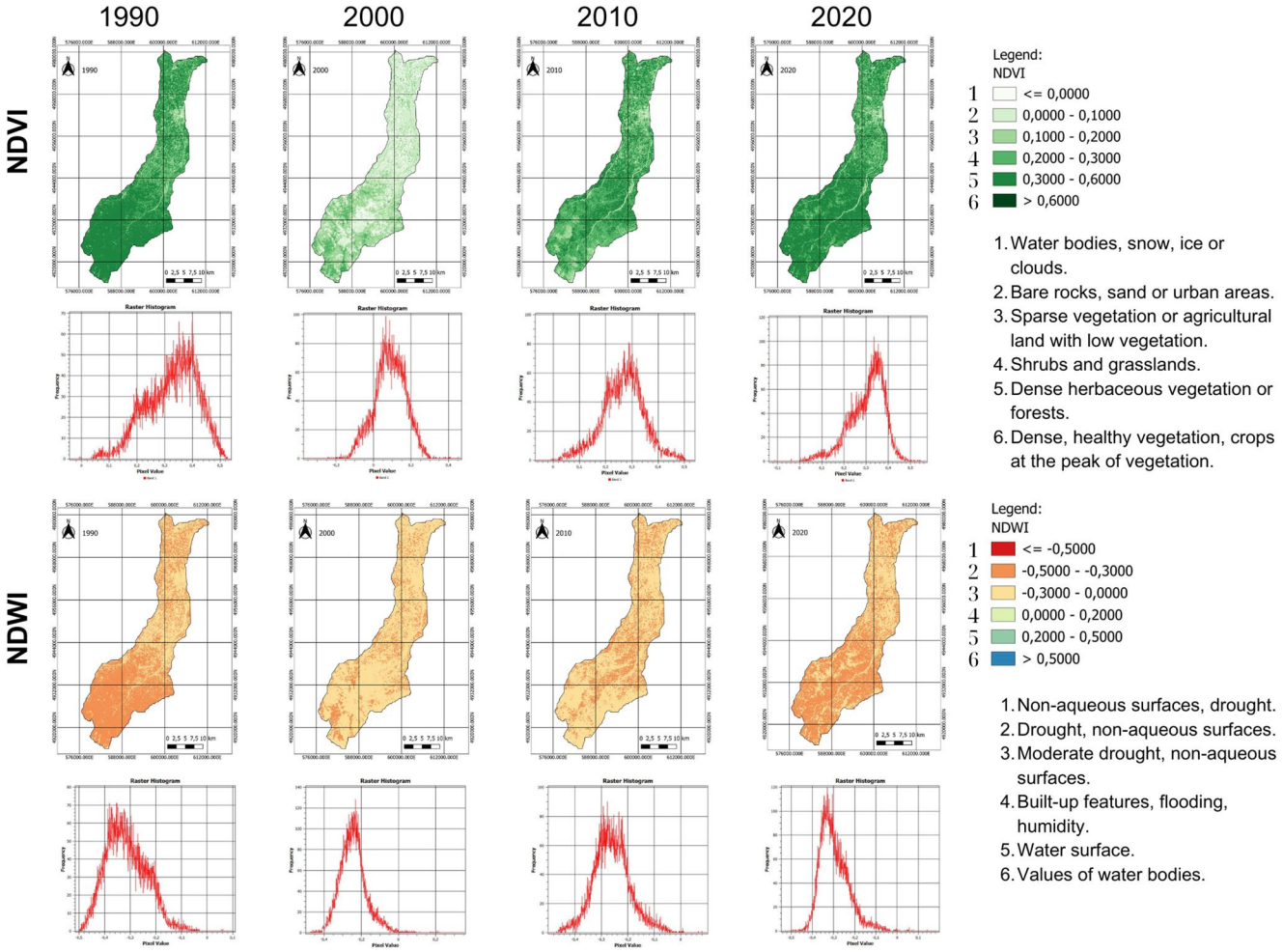

Fig. 5 Temporal changes in NDVI and NDWI of the Parma River basin. The figure illustrates spatial dynamics of NDVI (top panels) and NDWI (bottom panels) for the years 1990, 2000, 2010, and 2020. NDVI maps highlight changes in vegetation density and health, while NDWI maps represent variations in surface water presence. Raster histograms adjacent to each map show the pixel frequency distribution of index values

in the 2000 and 2020 data where larger areas display values between −0.5 and −0.3, indicating increased drought conditions. The spatial distribution of NDWI values has become more heterogeneous over time, suggesting uneven changes in water availability across the basin. The histograms demonstrate a progressive shift toward more negative values, indicating a general trend of decreasing water content in the basin's ecosystem.

Long-term trends in NDVI and NDWI in both river basins suggesting increased water stress over the past three decades, manifested differently in each geographical context. To better understand these dynamics and their potential drivers, we analyzed key climate indicators that directly affect vegetation condition and water availability in river ecosystems.

Statistical assessment of climate impact on vegetation dynamics

Two fundamental climate parameters were selected for analysis: (i) the Standardized Precipitation Index (SPI-6), which is a monthly index that compares accumulated precipitation for 6 months with the long-term precipitation distribution for the same location, and (ii) accumulation period, as the number of standard deviations from the mean and mean temperature, which is the mean of daily near-surface (2-meter) air temperature (Copernicus 2024). These indicators were chosen because they represent the primary climatic factors affecting both NDVI and NDWI values – SPI-6 directly influences water availability for vegetation and surface water bodies, while temperature affects evapotranspiration rates and overall water stress in ecosystems.

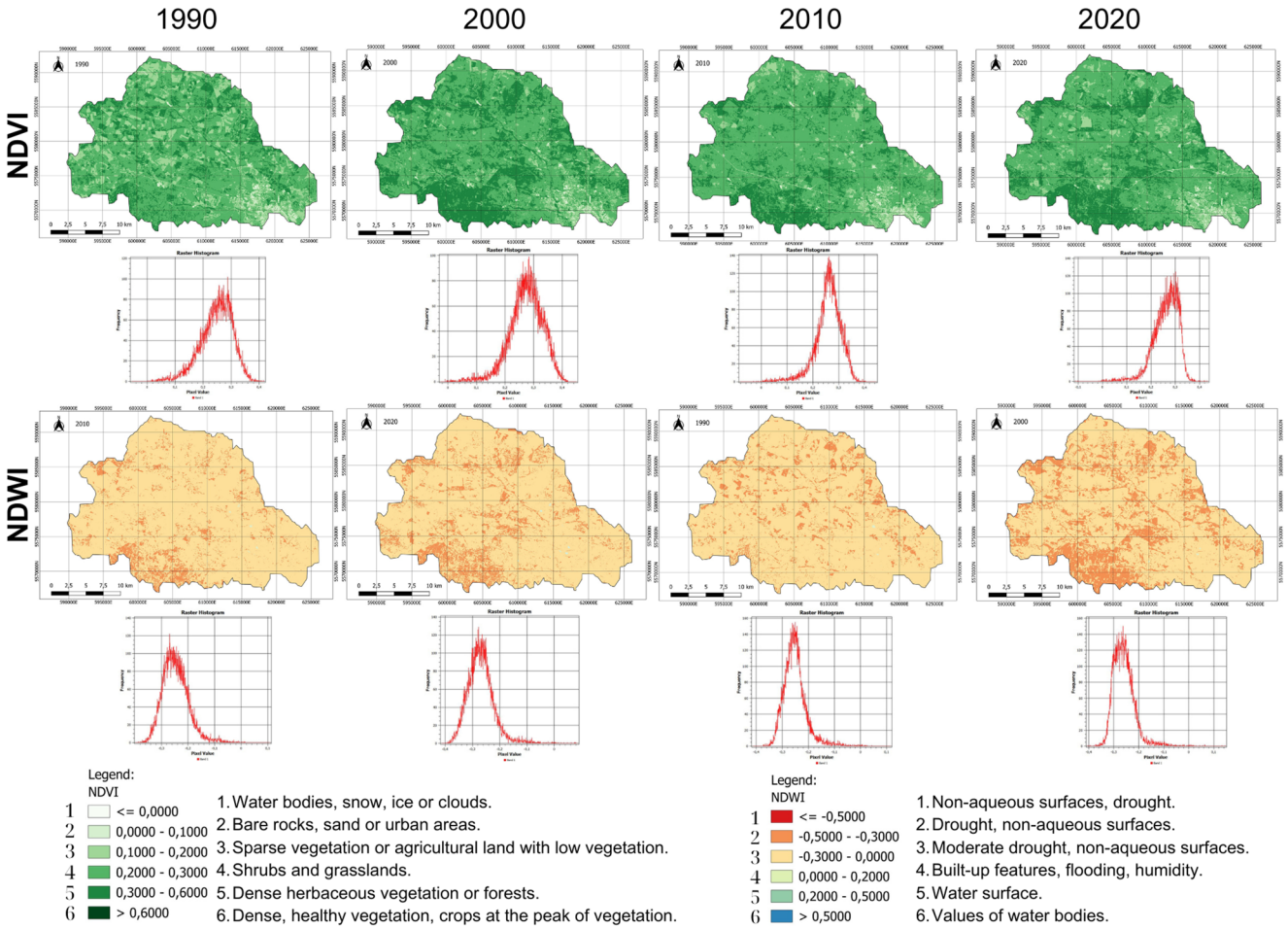

Fig. 6 Temporal changes in NDVI and NDWI of the Kamianka River basin. The figure illustrates the spatial distribution and pixel-based frequency histograms of the NDVI in the top panels and the NDWI in the bottom panels for four selected years: 1990, 2000, 2010, and 2020. NDVI maps highlight changes in vegetation density and health, while NDWI maps represent variations in surface water presence. Raster histograms adjacent to each map show the pixel frequency distribution of index values

The SPI-6 and mean temperature

The climate analysis for both regions reveals distinct trends, as illustrated in Figs. 7 and 8. For Italy's Parma River basin, the mean temperature shows a clear upward trend from 12.66°C in 1990 to 13.69°C in 2020, with an R^2 = 0.5759 indicating a strong warming trend. The SPI-6 values demonstrate significant variability, ranging from −0.92368 to 0.12779, with a positive trend y=0.0204x−40.872, R^2 = 0.1695, suggesting an increase in precipitation with high interannual variability (Fig. 7).

For Ukraine's Kamianka River basin, the mean temperature increase is pronounced, rising from 9.35°C to 10.75°C (y=0.0616x−114.42; R^2 = 0.5249), indicating a stronger warming trend compared to the Parma River basin. The SPI-6 exhibits a negative trend (y=−0.0188x+37.5, R^2 = 0.1487) ranging from −0.07259 to −0.96789, indicating a decreased precipitation over the study period (Fig. 8).

These graphs demonstrate that both regions are experiencing warming, but with different intensities and precipitation patterns: Italy shows trends toward increases in both temperature and SPI-6, while Ukraine exhibits more pronounced warming coupled with a decrease in SPI-6.

Correlation analysis between climate parameters and vegetation indices

To understand how these climate trends affect vegetation and water availability in both river basins, we conducted a correlation analysis between climate parameters and vegetation indices for the selected observation years within the 1990–2020 comparison period (Table 2).

Since only four representative years of observations were available for the correlation analysis, these relationships should be interpreted as indicative rather than statistically significant.

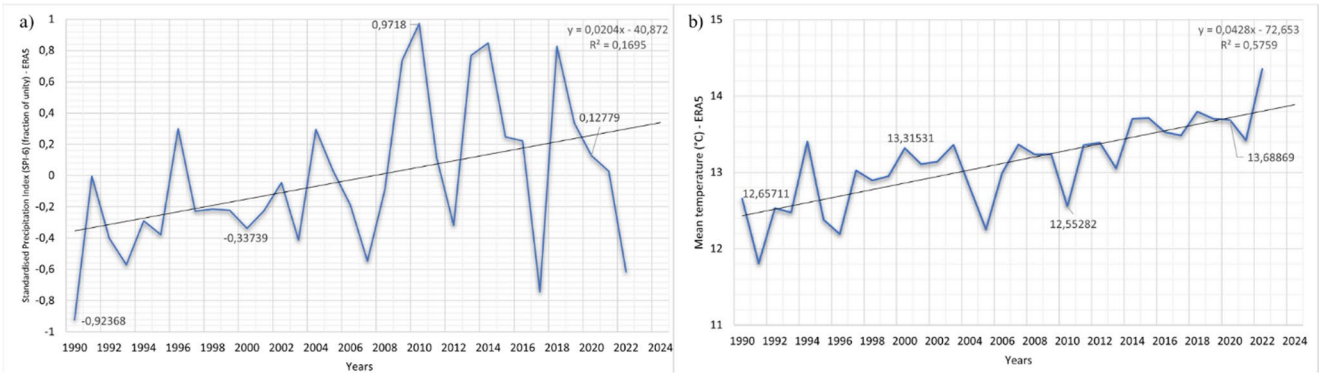

Fig. 7 Retrospective climate data for Italy from 1990 to present: a – shows interannual variation in the SPI-6, with a positive trend, indicating increasing precipitation and high interannual variability; b – shows the trend in annual mean air temperature, which increased over the study period. The corresponding regression indicates a strong warming trend in the basin. Both datasets are based on ERA5 reanalysis and reflect long-term climatic dynamics relevant to vegetation and water availability in the region

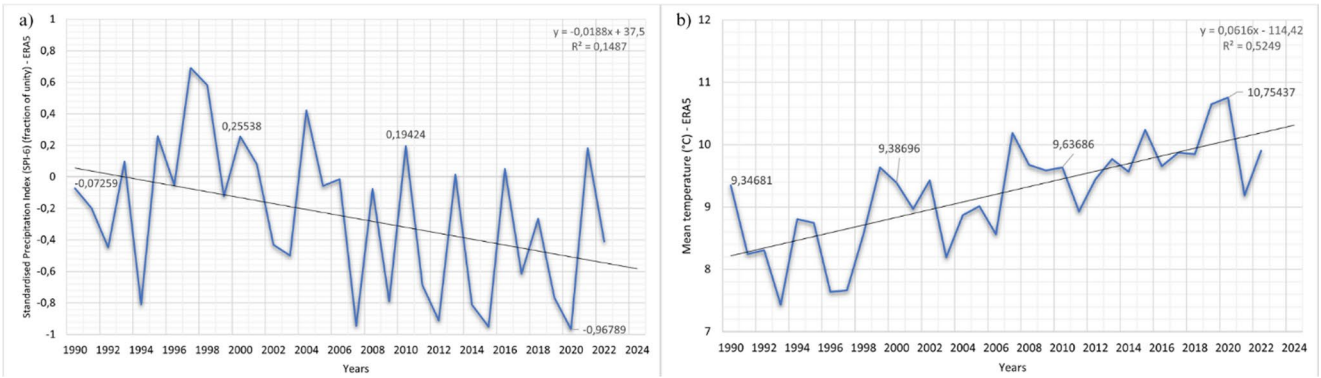

Fig. 8 Retrospective climate data for Ukraine from 1990 to present: a – shows interannual variation in the SPI-6, with a negative trend, indicating decreased precipitation. b – shows the trend in annual mean air temperature, which increased over the study period. The corresponding regression indicates a strong warming trend in the basin. Both datasets are based on ERA5 reanalysis and reflect long-term climatic dynamics relevant to vegetation and water availability in the region

Table 2 Pearson correlation coefficients between climatic variables (temperature, SPI-6) and vegetation indices (NDVI, NDWI) for the Parma and Kamianka river basins for selected years of observation (1990, 2000, 2010, 2020)

Parameters	Parma River basin	Kamianka River basin
Temperature vs. NDVI	−0.71	−0.82
Temperature vs. NDWI	−0.78	−0.85
SPI-6 vs. NDVI	0.65	0.61
SPI-6 vs. NDWI	0.73	0.69

Correlations are based on four years of observations (1990, 2000, 2010, 2020) and are reported as exploratory

The analysis employed the Pearson correlation coefficient (r), calculated as formula 4:

$$r = \frac{\sum \left((x_i - \overline{x}) (y_i - \overline{y}) \right)}{\sqrt{\sum (x_i - \overline{x})^2 \left(\sum (y_i - \overline{y}) \right)^2}} \quad (4)$$

where: r – pearson correlation coefficient, x_i – values of variable x, $\bar{x}$ – mean value of variable x, y_i – values of variable y, $\bar{y}$ – mean value of variable y, Σ – sum across all observations.

Since the correlation analysis was based on data from four representative years of observation (1990, 2000, 2010, and 2020), the calculated Pearson correlation coefficients should be considered preliminary rather than confirmatory. Due to the limited sample size, no formal hypothesis testing was conducted, and confidence intervals were not calculated; therefore, the results are intended to describe general patterns rather than establish statistically significant relationships.The correlation analysis shows differences between basins. In the Kamianka River basin, temperature is more strongly and negatively correlated with NDVI and NDWI than in the Parma River basin, indicating higher sensitivity

Table 3 Climate indicators and dominant NDVI and NDWI class intervals (annual seasonal mean) for the Parma River basin across selected years

Year	Average Temperature (°C)	SPI-6	Dominant NDVI class intervals	Dominant NDWI class intervals
1990	12.66	0.92	0.3 to 0.4	−0.2 to −0.1
2000	13.32	0.34	0.1 to 0.2	−0.3 to −0.2
2010	12.55	0.97	0.3 to 0.6	−0.2 to −0.1
2020	13.69	0.13	0.3 to 0.6	−0.3 to −0.2

Key findings - temperature: +1.03°C (12.66°C→13.69°C); precipitation (SPI-6): increasing trend; *NDVI* moderate improvement, *NDWI* moderate decrease

Table 4 Climate indicators and dominant NDVI and NDWI class intervals (annual seasonal mean) for the Kamianka River basin across selected years

Year	Average Temperature (°C)	SPI-6	Dominant NDVI class intervals	Dominant NDWI class intervals
1990	9.35	0.07	0.3 to 0.4	−0.2 to −0.1
2000	9.39	0.26	0.4 to 0.5	−0.3 to −0.2
2010	9.64	0.19	0.5 to 0.6	−0.2 to −0.1
2020	10.75	−0.97	0.4 to 0.5	−0.3 to −0.2

Key findings - temperature: +1.4 °C (9.35 °C→10.75 °C); precipitation (SPI-6): decreasing trend; *NDVI* significant improvement, *NDWI* noticeable decrease

to temperature variability. In both basins, SPI-6 is positively impact on NDVI and NDWI, with stronger SPI-6 relationships in the Parma River basin (Table 2).

These patterns align with the observed climate trends: the Kamianka River basin's stronger negative temperature correlations correspond to its more pronounced warming trend, while the Parma River basin's higher SPI-6 correlations reflect its greater sensitivity to precipitation variability. Overall, both basins exhibit different climatic and ecosystem responses that correspond to their contrasting geographical and ecological conditions.

The quantitative assessment of climate change impacts on both river basins reveals distinct ecosystem responses across the selected years. Based on the representative data summarized in Table 3, the Parma River basin experienced a moderate increase in mean annual temperature by 1.03°C (from 12.66°C in 1990 to 13.69°C in 2020), consistent with the trend shown in Fig. 7. The SPI-6 index showed significant variability over the selected years, with the lowest value recorded in 2020.The vegetation response (NDVI), summarized as the dominant class interval of the annual seasonal mean range, showed improvement, maintaining values between 0.3 and 0.6 in recent decades, although a notable decrease was observed in 2000 from 0.1 to 0.2. NDWI values indicated a decrease in water content, fluctuating between −0.3 and −0.1 throughout the study period.

The Kamianka River basin (Table 4) exhibited more pronounced changes in climate parameters. The temperature increase was more substantial, rising by 1.4°C from 9.35°C to 10.75°C over the study period. The precipitation trend, represented by SPI-6, showed a significant decline from 0.07 in 1990 to −0.97 in 2020, indicating increasingly dry conditions. Interestingly, despite these climatic pressures, the dominant NDVI class interval demonstrated significant improvement, increasing from 0.3 to 0.4 in 1990 to consistently higher values 0.4–0.6 in subsequent decades. However, the dominant NDWI class intervals showed a noticeable decrease, particularly evident in the fluctuations between −0.2 to −0.1 and −0.3 to −0.2, suggesting increased water stress in the ecosystem.

Statistical analysis suggests that climate-vegetation relationships are stronger in the Kamianka River basin than in the Parma River basin **(**Table 2**)**, indicating higher sensitivity to climatic variability in the Eastern European ecosystem. Despite stronger climatic stress, the Kamianka River basin shows more pronounced improvements in vegetation conditions compared with the more moderate improvement in the Parma River basin **(**Tables 3 and 4**)**, which suggests different adaptation mechanisms across ecoregions.

Discussion

These findings support the exploratory correlation analysis and demonstrate how climate change affect river ecosystems differently across climatic regions. Contrasting NDVI and NDWI responses to climatic variability highlight the complexity of ecosystem behavior and the need for basin-specific management.

It should also be noted that vegetation dynamics can be influenced not only by climatic factors, but also by changes in land use, agricultural practices, ecological succession, and local management measures. Therefore, the observed relationships should not be interpreted as being driven exclusively by climatic factors.

Our results align with previous research showing that river systems respond variably based on climate and ecoregion. For example, Parajka et al. (2013) found higher

predictability in humid basins, these findings are consistent with the stable patterns observed in the Parma basin. Conversely, the Kamianka basin's higher sensitivity supports Ranjbar et al. (2018) findings on arid basin vulnerability.

The NDVI increase, particularly in the stressed Kamianka basin, echoes Lu et al. (2021) and Gogoi and Rawat (2024), who showed that vegetation may adapt positively under certain conditions. However, lower NDWI conditions in the later observation years in both basins supports Pechlivanidis et al. (2017), who forecast growing water stress in transitional climates.

The observed increase in the NDVI index in the Kamyanka River basin, despite intensifying climate stress, may indicate the combined effect of vegetation adaptation and other ecological factors that were not clearly quantified in this study.

The use of GIS and satellite indices such as NDVI and NDWI has proven to be very effective in capturing temporal and spatial environmental changes, as confirmed by Nones (2021) and Langat et al. (2019). Our methodological framework further supports the usefulness of such technologies for comparative analysis, building on approaches tested in studies of the Vistula and Tana rivers.

Furthermore, the differences observed between the two basins reflect previous comparative studies, such as those by Wang et al. (2017) and Hattermann et al. (2017), which emphasized the value of regional models over global ones for identifying impacts at the basin level. This supports our conclusion that basin-specific adaptation strategies are needed, especially in contrasting ecozones such as the Mediterranean and Eastern European plains.

The Parma River basin, characterized by warming and variable precipitation, requires improvements in flood management, vegetation corridor resilience and adaptive water strategies, especially in years when the dominant NDVI class interval falls within 0.1 and 0.2, indicating vegetation stress. The Kamianka River basin, which is under more severe climate pressure, requires measures to mitigate the effects of drought, improve water retention infrastructure, and targeted analysis of how vegetation continues to adapt despite stress – an issue that warrants further research.

Future research should prioritize vegetation resilience mechanisms, basin-specific climate modeling, land-use impacts, cross-regional comparisons, monitoring of ecosystem services, remote sensing integration, and identification of potential ecological tipping points. When interpreting indicators derived from satellite data, one should also consider the uncertainties associated with remote sensing products and climate reanalysis datasets. However, the consistent patterns observed in both study basins suggest that the identified trends are ecologically significant, despite these methodological limitations. These research priorities would significantly enhance our understanding of river basin responses to climate change while supporting the development of more effective and scientifically grounded management strategies.

The results obtained may also contribute to the development of region-specific adaptation strategies within the framework of river basin management. The observed differences between the Parma and Kamianka river basins indicate that adaptation measures should take local climatic and environmental conditions into account, rather than relying on a universal upproach management approach. Thus, satellite monitoring can serve as a useful tool for identifying vulnerable areas and supporting long-term environmental planning.

Conclusions

This study suggests that climate change affects river basins differently depending on regional climatic and ecological conditions. Across the selected observation years (1990–2020), the Parma River basin experienced variable precipitation and moderate vegetation stability, while the Kamianka River basin experienced drying trends and signs of vegetation stress resistance.

Differences in NDVI and NDWI dynamics highlight the need for region-specific monitoring and adaptive strategies. The results confirm the effectiveness of satellite methods for assessing long-term ecosystem changes and provide a solid basis for future comparative analysis and improved, context-sensitive river basin management.

Since the analysis was based on representative years of observations, future studies should use longer, continuous satellite time series and additional environmental variables to further improve the reliability of comparative climate assessments. Future studies should cover longer observation periods, additional river basins, and field ecological measurements in order to further verify the identified relationships and enhance the reliability and applicability of the proposed methodological framework.

Authors' contributions All authors contributed to the study conception and design. Anna Kireitseva and Olha Shomko developed the research concept and methodology and collected the data. Olha Shomko calculated indexes in QGIS and prepared all illustrations. Anna Kireitseva analyzed and interpreted the results and wrote the first draft of the manuscript. Elena Maestri (corresponding author) and Irina Davydova reviewed and edited the manuscript and gave final approval for publication.

Funding Open access funding provided by Università degli Studi di Parma within the CRUI-CARE Agreement. The work was developed during a staff exchange in Erasmus+ project 2022-1-IT02-KA171-HED-000069814. Author Olha Shomko is supported by a fellowship of the University of Parma D.R. 597/2022.

Data availability All datasets used in this study are publicly available. Landsat Collection 2 Level 2 surface reflection images (1990, 2000, 2010, 2020, and 2023) were obtained from the USGS archive. URL: [https://earthexplorer.usgs.gov/](https://earthexplorer.usgs.gov). Basin boundaries and river network data were obtained from HydroSHEDS products (BasinATLAS and RiverATLAS). URL: https://www.hydrosheds.org/hydroatlas. SRTM digital elevation model (DEM) data were obtained from NASA. URL: [https://www.earthdata.nasa.gov/](https://www.earthdata.nasa.gov). Air temperature data at a height of 2 m was downloaded from the Copernicus Interactive Climate Atlas (C3S Atlas). The underlying grid dataset on which the C3S Atlas is based is available in the Copernicus Climate Data Store (CDS) under the name "Grid dataset underlying the Copernicus Interactive Climate Atlas". SPI-6 data were obtained from the Copernicus Climate Data Store (CDS) as "Monthly drought indices from 1940 to present, derived from reanalysis of ERA5 (ERA5–Drought)". Copernicus Interactive Climate Atlas URL: https://atlas.climate.copernicus.eu/atlas. Derivative products of NDVI/NDWI and supporting data obtained during this study can be obtained from Olha Shomko and Hanna Kireitseva upon reasonable request.

Declarations

Ethics declarations All authors give consent for submission and subsequent publication of the manuscript.

Competing interests The authors declare no competing interests.

Open Access This article is licensed under a Creative Commons Attribution 4.0 International License, which permits use, sharing, adaptation, distribution and reproduction in any medium or format, as long as you give appropriate credit to the original author(s) and the source, provide a link to the Creative Commons licence, and indicate if changes were made. The images or other third party material in this article are included in the article's Creative Commons licence, unless indicated otherwise in a credit line to the material. If material is not included in the article's Creative Commons licence and your intended use is not permitted by statutory regulation or exceeds the permitted use, you will need to obtain permission directly from the copyright holder. To view a copy of this licence, visit http://creativecommons.org/licenses/by/4.0/.

References

Abdelkader M, Bravo Mendez JH, Temimi M et al (2024) A Google Earth Engine platform to integrate multi-satellite and citizen science data for the monitoring of river ice dynamics. Remote Sens 16(8):1368. https://doi.org/10.3390/rs16081368

Arnell NW, Gosling SN (2016) The impacts of climate change on river flood risk at the global scale. Clim Change 134:387–401. https://doi.org/10.1007/s10584-014-1084-5

Chen SA, Michaelides K, Grieve SWD, Singer MB (2019) Aridity is expressed in river topography globally. Nature 573:573–577. https://doi.org/10.1038/s41586-019-1558-8

Copernicus (2024) European Climate Data Store. https://atlas.climate.copernicus.eu/atlas. Accessed 26 Jul 2024

De Rosa P, Fredduzzi A, Cencetti C (2024) Geographic information system tools for river evolution analysis. Water 16(17):2512. https://doi.org/10.3390/w16172512

EOS (2024) EOS Data Analytics. https://eos.com/. Accessed 15 Jul 2024

FAO (2024) Food and Agriculture Organization of the United Nations. https://www.fao.org/home/en/. Accessed 11 Oct 2024

Geoportal (2024) Regione Emilia-Romagna Geoportal. https://geoportale.regione.emilia-romagna.it/. Accessed 24 Jul 2024

Gogoi T, Rawat MS (2024) Study on NDVI and NDWI change detection of Gai river basin, NEI using GIS and remote sensing. Ecol Environ Conserv 30:S431–S435. https://doi.org/10.53550/EEC.2024.v30i05s.067

Hattermann FF, Krysanova V, Gosling SN et al (2017) Cross-scale intercomparison of climate change impacts simulated by regional and global hydrological models in eleven large river basins. Clim Change 141:561–576. https://doi.org/10.1007/s10584-016-1829-4

Heidari H, Arabi M, Warziniack T, Kao SC (2020) Assessing shifts in regional hydroclimatic conditions of U.S. river basins in response to climate change over the 21st century. Earths Future. https://doi.org/10.1029/2020EF001657

HydroSHEDS (2024) HydroSHEDS Database. https://www.hydrosheds.org/hydroatlas. Accessed 22 Jul 2024

Jarihani AA, Callow J, Johansen K, Gouweleeuw B (2013) Evaluation of multiple satellite altimetry data for studying inland water bodies and river floods. J Hydrol (Amst) 505:78–90. https://doi.org/10.1016/j.jhydrol.2013.09.010

Langat PK, Kumar L, Koech R (2019) Monitoring river channel dynamics using remote sensing and GIS techniques. Geomorphology 325:92–102. https://doi.org/10.1016/j.geomorph.2018.10.007

Lu C, Hou M, Liu Z et al (2021) Variation Characteristic of NDVI and its Response to Climate Change in the Middle and Upper Reaches of Yellow River Basin, China. IEEE J Sel Top Appl Earth Obs Remote Sens 14:8484–8496. https://doi.org/10.1109/JSTARS.2021.3105897

NASA (2024) Earth Data NASA. https://www.earthdata.nasa.gov/. Accessed 20 Jul 2024

Nones M (2021) Remote sensing and GIS techniques to monitor morphological changes along the middle-lower Vistula river, Poland. Int J River Basin Manage. https://doi.org/10.1080/15715124.2020.1742137

Parajka J, Viglione A, Rogger M et al (2013) Comparative assessment of predictions in ungauged basins-Part 1: runoff-hydrograph studies. Hydrol Earth Syst Sci 17:1783–1795. https://doi.org/10.5194/hess-17-1783-2013

Pechlivanidis IG, Arheimer B, Donnelly C et al (2017) Analysis of hydrological extremes at different hydro-climatic regimes under present and future conditions. Clim Change 141:467–481. https://doi.org/10.1007/s10584-016-1723-0

Ranjbar S, Hooshyar M, Singh A, Wang D (2018) Quantifying climatic controls on river network branching structure across scales. Water Resour Res 54:7347–7360. https://doi.org/10.1029/2018WR022853

Sulistioadi YB, Tseng KH, Shum CK et al (2015) Satellite radar altimetry for monitoring small rivers and lakes in Indonesia. Hydrol Earth Syst Sci 19:341–359. https://doi.org/10.5194/hess-19-341-2015

Wang X, Yang T, Wortmann M et al (2017) Analysis of multidimensional hydrological alterations under climate change for four major river basins in different climate zones. Clim Change 141:483–498. https://doi.org/10.1007/s10584-016-1843-6

Wang H, Liu J, Klaar M et al (2024) Anthropogenic climate change has influenced global river flow seasonality. Science 383:1009–1014. https://doi.org/10.1126/science.adi9501

WFD (2024) Water Framework Directive. https://environment.ec.europa.eu/topics/water/water-framework-directive_en. Accessed 20 Jul 2024

Publisher's note Springer Nature remains neutral with regard to jurisdictional claims in published maps and institutional affiliations.